

Instanton correlators and phase transitions in two- and three-dimensional logarithmic plasmas

K. Børkje,^{1,*} S. Kragset,^{1,†} and A. Sudbø^{1,‡}

¹*Department of Physics, Norwegian University of Science and Technology, N-7491 Trondheim, Norway*

(Dated: September 19, 2018)

The existence of a discontinuity in the inverse dielectric constant of the two-dimensional Coulomb gas is demonstrated on purely numerical grounds. This is done by expanding the free energy in an applied twist and performing a finite-size scaling analysis of the coefficients of higher-order terms. The phase transition, driven by unbinding of dipoles, corresponds to the Kosterlitz-Thouless transition in the 2D XY model. The method developed is also used for investigating the possibility of a Kosterlitz-Thouless phase transition in a three-dimensional system of point charges interacting with a logarithmic pair-potential, a system related to effective theories of low-dimensional strongly correlated systems. We also contrast the finite-size scaling of the fluctuations of the dipole moments of the two-dimensional Coulomb gas and the three-dimensional logarithmic system to those of the three-dimensional Coulomb gas.

PACS numbers:

I. INTRODUCTION

Compact $U(1)$ gauge fields in three dimensions are of great interest in condensed matter theory, as they arise in effective theories of strongly correlated two-dimensional systems at zero temperature.^{1,2,3,4} Lightly doped Mott-Hubbard insulators, such as high- T_c cuprates, are examples of systems possibly described by such theories, where the compact gauge field emerges from strong local constraints on the electron dynamics.^{2,5,6,7} High- T_c cuprates appear to fall outside the Landau Fermi liquid paradigm, and a so-called confinement-deconfinement transition in the gauge theories may be associated with breakdown of Fermi-liquid and quasiparticles in 2D at $T = 0$.^{6,7,8} Obliteration of electron-like quasiparticles and spin-charge separation in the presence of interactions is well known to occur in one spatial dimension. However, the mechanism operative in that case, namely singular forward scattering, is unlikely to be operative in higher dimensions due to the much less restrictive kinematics at the Fermi surface.⁹ Proliferation of instantons of emergent gauge fields show more promise as a viable candidate mechanism. This line of pursuit has recently been reinvigorated in the context of understanding the physics of lightly doped Mott-Hubbard insulators and unconventional insulating states.¹⁰

The compact nature of a constraining gauge field on a lattice model introduces topological defects defined by surfaces where the field jumps by 2π , forming a gas of instantons (or "monopoles") in $2+1$ dimensions.¹¹ Considering the gauge sector only, the interactions between these instantonic defects are the same as between charges in a 3D Coulomb gas, *i.e.* $1/r$ -interactions. Such a gas is always in a metallic or plasma phase with a finite screening length,^{11,12} and there is no phase transition between a metallic regime and an insulating regime. However, in models where compact gauge fields are coupled to *matter fields*, the interaction between the magnetic monopoles may be modified by the emergence of

an anomalous scaling dimension of the gauge field due to critical matter-field fluctuations.¹³ This is the case for the compact abelian Higgs model with matter fields in the fundamental representation.¹⁴

In Refs. 14, it was shown that the introduction of a matter field with the fundamental charge leads to an anomalous scaling dimension in the gauge field propagator¹³. The effect is to alter the interaction potential between the magnetic monopoles from $1/r$ to $-\ln r$. The existence of a confinement-deconfinement transition in the gauge theory is thus related to whether a phase transition occurs in a 3D gas of point charges with logarithmic interactions. However, one should note that the legitimacy of a monopole action based on just pairwise interactions has been questioned, particularly when viewed as an effective description of an effective gauge theory of strongly interacting systems.¹⁵ The 3D logarithmic plasma is however of considerable interest in its own right.

In two dimensions, where $-\ln r$ is the Coulomb potential, it is known that the logarithmic gas experiences a phase transition from a low-temperature insulating phase consisting of dipoles to a high-temperature metallic phase. This is nothing but the Coulomb-gas representation of the Kosterlitz-Thouless transition in the 2D XY model. In a 3D logarithmic gas, the existence of a phase transition is still subject to debate.^{14,16,17} Renormalization group arguments have been used¹⁴ to demonstrate that a transition may occur, driven by the unbinding of dipoles. Others have claimed that the 3D logarithmic gas is always in the metallic phase.¹⁶ In a recent paper,¹⁸ large scale Monte Carlo simulations indicated that two distinct phases of the 3D-log gas exists; a low- T regime where the dipole moment does not scale with system size and a high- T regime where the dipole moment is system size dependent. Those results do however not determine the character of the phase transitions. That will be the main subject of this paper.

The Kosterlitz-Thouless transition in the 2D XY model

is characterized by the universal jump to zero of the helicity modulus.¹⁹ In the corresponding 2D Coulomb gas, it is the inverse of the macroscopic dielectric constant ϵ that experiences a jump to zero when going from the insulating to the metallic phase. According to Ref. 14, such a universal discontinuity should also take place for ϵ^{-1} in the 3D logarithmic gas associated with the confinement-deconfinement transition. Proving that such discontinuities exist numerically is a subtle task. The discontinuous character of the helicity modulus in the 2D XY model is very hard to see in a convincing manner by computing the helicity modulus, due to severe finite-size effects. It was only recently proven on purely numerical grounds that such a discontinuity exists²⁰ in a simple, but yet clever manner. By imposing a twist across the system and expanding the free energy in this twist to the fourth order, a stability argument was used to show that the second order term in the expansion, the helicity modulus, must be nonzero at T_c . The proof relies on the ability to conclude that the fourth order term is negative in the thermodynamic limit, from which the discontinuity follows immediately. In this paper, we will repeat this procedure, but now in the language of the 2D Coulomb gas. In addition to confirming the results of Minnhagen and Kim, the method which we develop here could be suitable for proving the possibly discontinuous behaviour of ϵ^{-1} in the 3D logarithmic gas. This is a main motivation for translating the procedure of Ref. 20 to the vortex language, since the 3D logarithmic gas is not the dual theory of any simple spin model. After having demonstrated the discontinuity in the 2D Coulomb gas, we go on to apply the method on the 3D logarithmic gas. We also compare the scaling with system size of the mean square dipole moment for these logarithmic plasmas, and contrast the results with those of the 3D Coulomb gas. This is important, since the mean square dipole moment does not scale with system size below a certain temperature for the logarithmic plasmas.¹⁸ This indicates that two phases exist, where the low-temperature regime consists of tightly bound pairs. However, the results for the 3D Coulomb gas are qualitatively different, in accordance with the fact that such a low-temperature phase is absent in that case.

II. MODEL

The Hamiltonian of the 2D XY model on a square lattice modified with a twist $\mathbf{T}(x, y)$ is

$$H_{XY} = -J \sum_{\langle i,j \rangle} \cos(\theta_i - \theta_j - 2\pi \mathbf{r}_{ij} \cdot \mathbf{T}), \quad (1)$$

where \mathbf{r}_{ij} is the displacement between the nearest neighbour pairs to be summed over. We set the coupling constant J to unity. The volume of the system, *i.e.* the number of lattice points, is L^2 , and the angle θ_i is subject to periodic boundary conditions. In the Villain approximation, a duality transformation leads to the Hamiltonian

$$H = \frac{1}{2} \sum_{i,j} (m_i + \varepsilon^{\mu\nu} \Delta^\mu T^\nu)_i V_{ij} (m_j + \varepsilon^{\rho\sigma} \Delta^\rho T^\sigma)_j, \quad (2)$$

where m_i are point charges on the dual lattice, corresponding to vortex excitations in the XY model. Δ^μ is a lattice derivative and $\varepsilon^{\mu\nu}$ is the completely antisymmetric symbol. The potential V_{ij} is given by

$$V(|\mathbf{r}_i - \mathbf{r}_j|) = \frac{2\pi^2}{L^2} \sum_{\mathbf{q}} \frac{e^{-i\mathbf{q} \cdot (\mathbf{r}_i - \mathbf{r}_j)}}{2 - \cos q_x - \cos q_y}, \quad (3)$$

which has a logarithmic long-range behaviour. Details of the dualization are found in appendix A. As is well known, eq. (2) at zero twist describes the two-dimensional Coulomb gas (2D CG). In this representation, the Kosterlitz-Thouless phase transition of the 2D XY model is recognized by a discontinuous jump to zero of the inverse macroscopic dielectric constant ϵ^{-1} at T_c . We note that the curl of the twist \mathbf{T} acts as a modification of the charge field in the 2D CG.

The free energy of the system is $F = -T \ln Z$, where the partition function is given by summing the Boltzmann factor over all charge configurations:

$$Z = \sum_{\{m\}} e^{-H/T}. \quad (4)$$

Let us write the Hamiltonian in Fourier representation,

$$H = \frac{1}{2L^2} \sum_{\mathbf{q}} (m_{\mathbf{q}} + \varepsilon^{\nu\lambda} Q_{-\mathbf{q}}^\nu T_{\mathbf{q}}^\lambda) V_{\mathbf{q}} (m_{-\mathbf{q}} + \varepsilon^{\rho\sigma} Q_{\mathbf{q}}^\rho T_{-\mathbf{q}}^\sigma), \quad (5)$$

where the discrete Fourier transform is defined as in appendix B and $\Delta^\mu e^{\pm i\mathbf{q} \cdot \mathbf{r}} \equiv e^{\pm i\mathbf{q} \cdot \mathbf{r}} Q_{\pm\mathbf{q}}^\mu$.

III. STABILITY ARGUMENT

From (1), it is clear that $F(\mathbf{T}) \geq F(0)$ in the low-temperature phase, *i.e.* the free energy is minimal for zero twist. This inequality is also valid at the critical temperature T_c , since the free energy must be a continuous function of temperature. As a consequence, the Taylor expansion

$$\begin{aligned} F(\mathbf{T}) - F(0) &= \sum_{\alpha} \sum_{\mathbf{q}_1} \left. \frac{\partial F}{\partial T_{\mathbf{q}_1}^\alpha} \right|_{\mathbf{T}=0} T_{\mathbf{q}_1}^\alpha \\ &+ \sum_{\alpha,\beta} \sum_{\mathbf{q}_1, \mathbf{q}_2} \left. \frac{\partial^2 F}{\partial T_{\mathbf{q}_1}^\alpha \partial T_{\mathbf{q}_2}^\beta} \right|_{\mathbf{T}=0} \frac{T_{\mathbf{q}_1}^\alpha T_{\mathbf{q}_2}^\beta}{2} + \dots \end{aligned} \quad (6)$$

can not be negative for any $T \leq T_c$. Expressions for the derivatives of the free energy with respect to a general twist are found in appendix B. Only terms of even order will contribute to the series, since m_i may take equally

many positive and negative values. We are free to *choose* the twist to be

$$\mathbf{T}(x, y) = \frac{\Delta}{L^\eta} \sin\left(\frac{2\pi y}{L}\right) \hat{\mathbf{x}}, \quad (7)$$

where Δ is an arbitrarily small constant and $\eta = 1$ for the two-dimensional Coulomb gas. To the fourth order, this long-wavelength twist turns (6) into

$$F(\mathbf{T}) - F(0) = \frac{\Delta^2}{4} C_{\mathbf{k}} \left(1 - \frac{V_{\mathbf{k}}}{L^2 T} \langle m_{\mathbf{k}} m_{-\mathbf{k}} \rangle\right) + \frac{\Delta^4}{32} \frac{(C_{\mathbf{k}} V_{\mathbf{k}})^2}{L^4 T^3} \left(\langle m_{\mathbf{k}} m_{-\mathbf{k}} \rangle^2 - \frac{1}{2} \langle (m_{\mathbf{k}} m_{-\mathbf{k}})^2 \rangle\right), \quad (8)$$

where $\mathbf{k} = (0, 2\pi/L)$ and $C_{\mathbf{k}} = Q_{\mathbf{k}}^y Q_{-\mathbf{k}}^y V_{\mathbf{k}}$. We recognize the paranthesis in the second order term as the dielectric response function $\epsilon^{-1}(\mathbf{k})$, where \mathbf{k} is now the smallest nonzero wave vector in a finite system. Note that the prefactors in both terms are independent of system size as $L \rightarrow \infty$. The crucial argument to use is the same as in Ref. 20. If the fourth order term approaches a finite negative value at T_c in the limit $L \rightarrow \infty$, the second order term, $\epsilon^{-1}(\mathbf{k} \rightarrow 0)$, must be positive to satisfy the inequality $F(\mathbf{T}) \geq F(0)$. Furthermore, since we know that the inverse dielectric constant is zero in the high-temperature phase, it necessarily experiences a discontinuity at T_c . As we shall see, Monte Carlo simulations show that the fourth order term is indeed negative at T_c in the thermodynamic limit.

The argument described above will also apply to a three-dimensional gas of point charges interacting via a pair potential of some sort, as long as the twist raises the free energy in the low-temperature regime. Since the curl of the twist \mathbf{T} is a vector in that case, one may for instance choose the z -component of this vector as the perturbing charge in eq. (2). The two three-dimensional systems we will consider are the logarithmic gas and the Coulomb gas. The expansion (6) is valid for any system size L . However, to make the change in free energy nondivergent as $L \rightarrow \infty$, the twist must be chosen such that the terms in the expansion are independent of system size. This is obtained by choosing $\eta = 2$ for the logarithmic gas and $\eta = 3/2$ for the Coulomb gas. η is defined in (7). In both cases, the second order term will be proportional to

$$\epsilon^{-1}(\mathbf{k}) = 1 - \frac{V_{\mathbf{k}}}{L^3 T} \langle m_{\mathbf{k}} m_{-\mathbf{k}} \rangle. \quad (9)$$

The fourth order term will be proportional to

$$\epsilon_4(\mathbf{k}) \equiv \frac{1}{T^3} \left(\langle m_{\mathbf{k}} m_{-\mathbf{k}} \rangle^2 - \frac{1}{2} \langle (m_{\mathbf{k}} m_{-\mathbf{k}})^2 \rangle \right) \quad (10)$$

in the logarithmic case. In the case of a 3D Coulomb gas, the interesting quantity will be ϵ_4/L^2 , which is independent of system size since $\langle m_{\mathbf{k}} m_{-\mathbf{k}} \rangle \sim L$ in that case.

IV. SIMULATION RESULTS

Standard Metropolis Monte Carlo simulations are carried out on the model (2) at zero twist. An $L \times L$ square lattice with periodic boundary conditions is used and the system is kept electrically neutral at all times during the simulations. This is achieved by inserting dipoles with probability according to the Metropolis algorithm: An insertion of a negative or positive charge is attempted at random at a given lattice site, and an opposite charge is placed at one of the nearest neighbour sites to make the dipole. This is one move, accepted with probability $\exp(-\Delta E/T) = \exp[-(\mathcal{H}_{\text{new}} - \mathcal{H}_{\text{old}})/T]$, and the sequence of trying this for all sites in the system once is defined as one sweep. If a charge is placed on top of an opposite one, the effect is to annihilate the existing one. All simulations are performed going from high to low temperature and after simulating one system size L the sampled data are postprocessed using Ferrenberg-Swendsen reweighting techniques.²¹

A. 2D Coulomb gas

We consider first the 2D Coulomb gas, which is known to suffer a metal-insulator transition via a Kosterlitz-Thouless phase transition. In this case, Monte Carlo data are obtained for $L = 4 - 100$ and for each L up to 200 000 sweeps at each temperature is used.

We start by taking the Hamiltonian (2) and computing the mean square of the dipole moment, $\langle s^2 \rangle$, as a function of system size and temperature. A mean square dipole moment which is independent of system size indicates the existence of tightly bound dipoles and a dielectric or insulating phase. If the mean square dipole moment scales with system size, this demonstrates the existence of free unbound charges and hence a metallic phase. In other words, we expect in the low-temperature dielectric insulating phase no finite-size scaling of $\langle s^2 \rangle$, whereas we should expect $\langle s^2 \rangle \propto L^{\alpha(T)}$ with $\alpha(T) \leq 2$ at higher temperatures. Using an intuitive low density argument, neglecting screening effects,²² we can calculate the behaviour of $\langle s^2 \rangle$ to leading order in L ,

$$\langle s^2 \rangle \propto \begin{cases} \text{Const.} & ; T < T_{KT} \\ L^{(T-T_{KT})/T} & ; T_{KT} < T < 2T_{KT} \\ L^2 & ; 2T_{KT} < T. \end{cases} \quad (11)$$

Hence, $\alpha(T)$ is zero for low temperatures and a monotonically increasing function of temperature just above T_{KT} . Including screening effects in 2D shows that this conclusion still holds, however the temperature at which it occurs is determined by screening.

Details of the simulations may be found in Ref. 18. The result is shown in Fig. 1 where we have the mean square dipole moment for the 2D case both as a function of temperature for various system sizes, and as function of system size for various temperatures. From this we

may extract the scaling constant $\alpha(T)$ which is shown in the center panel of Fig. 1. A related method for using dipole fluctuations to measure vortex-unbinding has recently been used in Refs. 23.

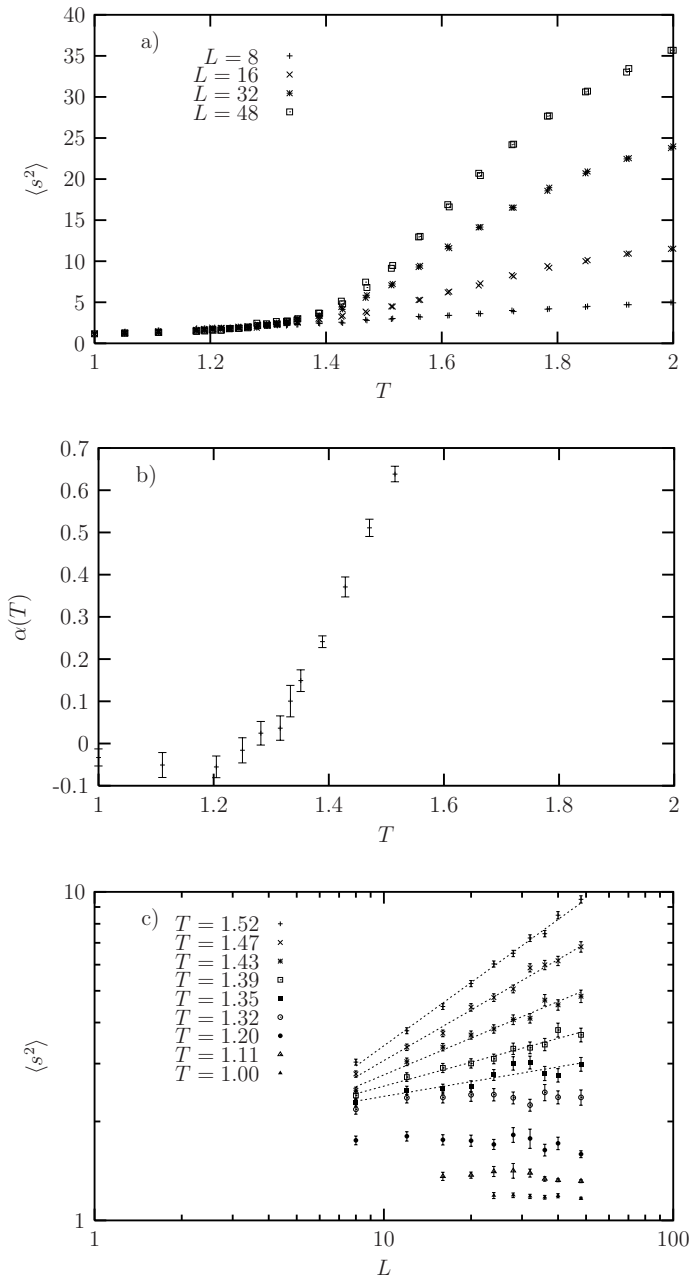


FIG. 1: The mean square dipole moment $\langle s^2 \rangle$ as a function of temperature (top panel), and system size (bottom panel) for the 2D Coulomb gas. The middle panel shows the scaling exponent α extracted from $\langle s^2 \rangle \sim L^{\alpha(T)}$.

Below a temperature $T \approx 1.3$, no scaling of $\langle s^2 \rangle$ is seen, consistent with a low-temperature dielectric phase. The temperature at which scaling stops is consistent with the known temperature at which the 2D Coulomb gas suffers a metal-insulator transition.

Simulation results for the inverse dielectric constant

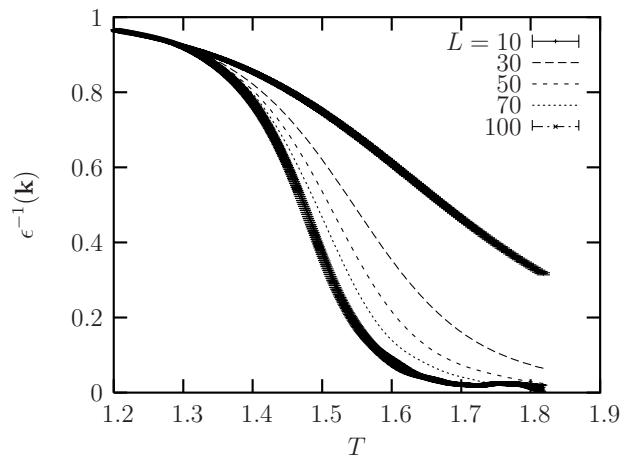


FIG. 2: Inverse dielectric constant taken at the smallest possible wave vector in a finite system, $\mathbf{k} = (0, 2\pi/L)$, and plotted against temperature T for system sizes $L = 10, 30, 50, 70$ and 100 , for the 2D Coulomb gas. The decrease of ϵ^{-1} towards zero becomes sharper with increasing L , consistent with the prediction of a discontinuous jump. Errorbars are given in the top and bottom curves, and omitted for clarity in the others.

are shown for a selection of system sizes in Fig. 2. Since ϵ^{-1} is expected to be discontinuous at T_c in the limit $\mathbf{k} \rightarrow 0$, we consider only the smallest possible wave vector in each system, $\mathbf{k} = (0, 2\pi/L)$, and we see that the decrease of ϵ^{-1} towards zero with increasing T indeed gets sharper as L grows. It is however difficult to decide from these plots alone whether or not the dielectric constant is discontinuous at T_c . The fourth order term in the expansion of the free energy, ϵ_4 defined in eq. (10), is therefore investigated in a corresponding manner and plotted in Fig. 3.

We note that this quantity has a dip at a temperature which can be associated with the transition temperature. If this dip remains finite and negative as L approaches infinity, ϵ^{-1} must exhibit a jump at T_c . The depth of the dip is shown in Fig. 4 for a variety of system sizes ranging from $L = 4$ to $L = 100$ and as a function of $1/L$. It clearly decreases with increasing L . However, from the positive curvature of the data in the log-log plot we may conclude that the depth remains nonzero when we extrapolate to $1/L = 0$, a conclusion reached by assuming power-law dependence of the depth on L .

We can now subtract from the depth a constant chosen so as to linearize the curve in the log-log plot. This constant consequently corresponds to the depth when extrapolating the data to the thermodynamic limit $1/L = 0$, and we find this to be 0.047 ± 0.005 .

By plotting the temperature at which the fourth order term has its minimum against $1/L$, we can follow a similar procedure as the above one. This is shown in Fig. 5. We linearize a log-log plot by subtracting a carefully chosen constant and end up with the number 1.36 ± 0.04 . This is nothing else than an estimate of the critical temperature of the 2D CG, and compares well to

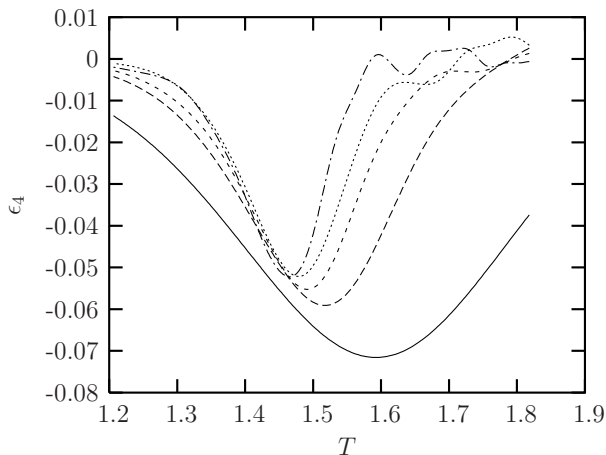


FIG. 3: The coefficient ϵ_4 of the fourth order term of the expansion of the free energy, for the 2D Coulomb gas. The same systems are used in this plot as in Figure 2, and the depths decrease with increasing L . The important question is whether this dip vanishes at T_c or not. Errorbars are omitted but will be reintroduced in Figure 4. The oscillation at high T is due to noise from the reweighting.

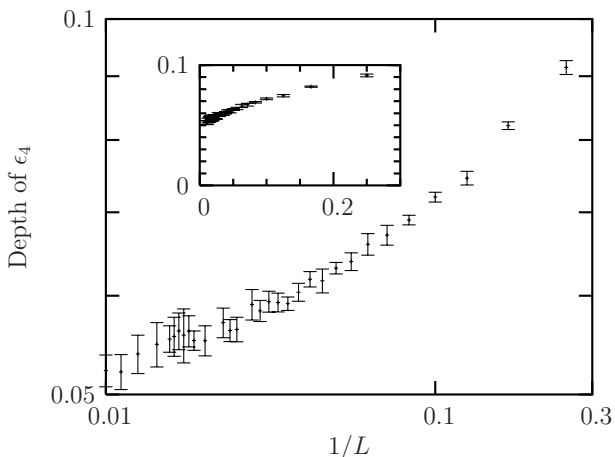


FIG. 4: Depth of the dip in the fourth order term shown in Figure 3 for the 2D Coulomb gas. The data are obtained from simulations of system sizes ranging from $L = 4$ to $L = 100$ and plotted both on a linear scale (inset) and on a log-log scale. The positive curvature in the log-log plot clearly indicates a nonzero value of the depth when extrapolating to the limit $L \rightarrow \infty$.

earlier results.²⁴ The approach towards T_c is however a bit slow, making a precise determination of the critical temperature difficult. This drawback was also noted by Minnhagen and Kim for the corresponding computations on the 2D XY model.²⁰

B. 3D logarithmic system

We may carry out the same type of analysis for the mean square dipole moment for a system of point charges

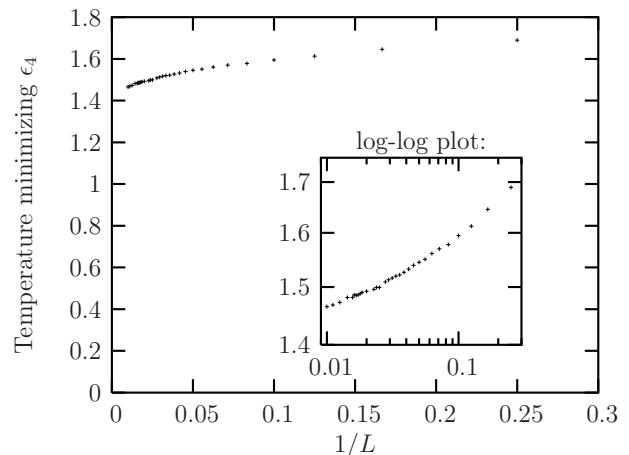


FIG. 5: Temperature minimizing ϵ_4 as a function of inverse system size for the 2D CG. The values are plotted both on a linear scale and on a log-log scale (inset). This temperature reaches a nonzero value at $L \rightarrow \infty$ indicated by the positive curvature in the log-log plot. Extrapolation gives $T_c = 1.36 \pm 0.04$.

interacting via a three-dimensional logarithmic bare pair potential (3D LG). For this system, much less is known. Such a system has recently been considered in the context of studying confinement-deconfinement phase transitions in the $(2+1)$ -dimensional abelian Higgs model.¹⁴ The results are shown in Fig. 6.

Qualitatively and quantitatively the results are the same in the 3D LG as for the 2D case. This strongly suggests that the 3D LG also has a low-temperature dielectric insulating phase separated by a phase transition from a high-temperature phase. In the low-temperature regime the charges of almost all dipoles are bound as tightly as possible, the separation of the charges correspond to the lattice constant. In the high-temperature regime the dipoles have started to separate, reflected by a scaling of $\langle s^2 \rangle \sim L^{\alpha(T)}$ with the system size. Since $\alpha(T) = 0$ at low temperatures while $\alpha(T) \neq 0$ in the high-temperature regime a non-analytic behaviour of $\alpha(T)$ is implied. This necessarily corresponds to a phase transition in the vicinity of $T \approx 0.3$, a temperature which agrees well with Ref. 14 where a critical value of $T_c = 1/3$ was obtained.

Note that, although this simple type of analysis of the mean square dipole moment does not by itself suffice to determine the character of these phase transitions either in the case of 3D LG or 2D CG, it does suffice to shed light on the important issue of whether a low temperature insulating phase exists in the 3D LG as well. This is far from obvious, since the screening properties of a three-dimensional system of charges interacting logarithmically is quite different from that of a Coulomb system (in any dimension).¹⁶ It is therefore of considerable interest to repeat the analysis carried out for the 2D Coulomb gas to, if possible, determine the character of a metal-insulator transition in the 3D LG.

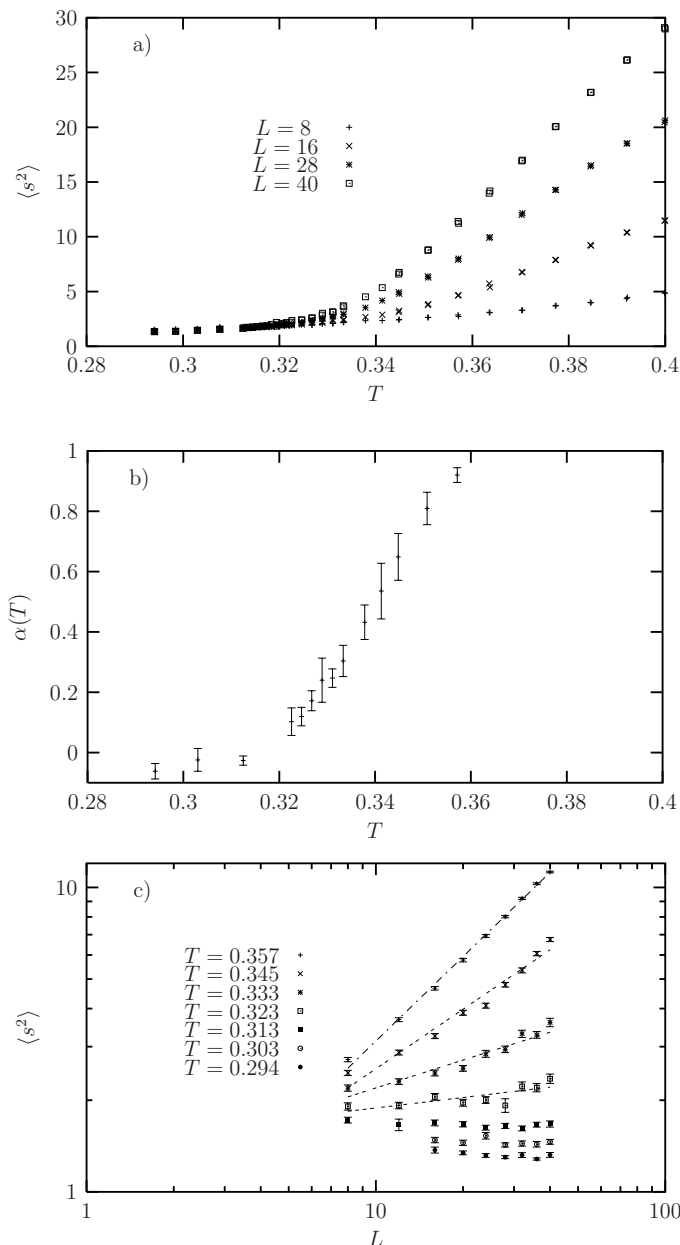


FIG. 6: Mean square dipole moment $\langle s^2 \rangle$ as a function of temperature (top panel) and system size (bottom panel) for the 3D system of point charges interacting with a logarithmic bare pair potential (3D LG). The middle panel shows the scaling exponent α extracted from $\langle s^2 \rangle \sim L^{\alpha(T)}$.

In Fig. 7 we show the inverse dielectric constant for the 3D LG as a function of temperature for various system sizes. It shows qualitatively the same behavior as for the 2D CG in that the decrease of ϵ^{-1} towards zero becomes sharper with increasing L . However, the downward drift in the temperature at which the inverse dielectric constant starts decreasing rapidly is more pronounced than in the 2D CG case.

In Fig. 8 we have plotted the fourth order coefficient against temperature for the 3D LG system, and the depth

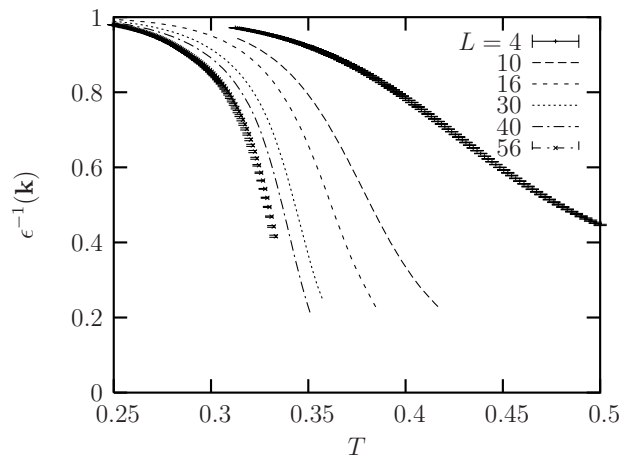


FIG. 7: Inverse dielectric constant taken at the smallest possible wave vector in a finite system, $\mathbf{k} = (0, 2\pi/L, 0)$, and plotted against temperature T for system sizes $L = 4, 10, 16, 30, 40$ and 56 , for the 3D LG system. The decrease of ϵ^{-1} towards zero becomes sharper with increasing L , consistent with the prediction of a discontinuous jump. However, the downward drift in the temperature at which the inverse dielectric constant starts decreasing rapidly is more pronounced than in the 2D CG case. Errorbars are given in the top and bottom curves, and omitted for clarity in the others.

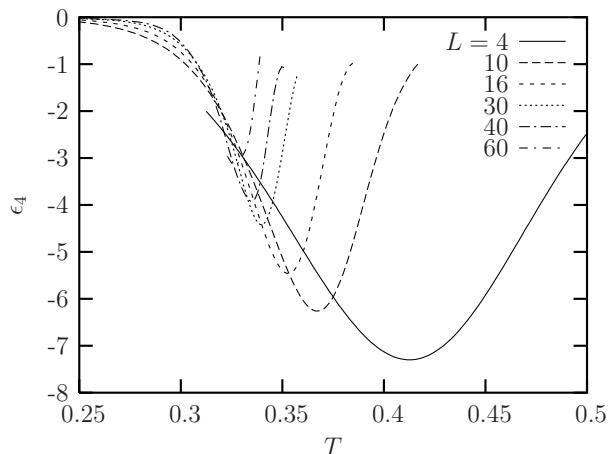


FIG. 8: The coefficient ϵ_4 of the fourth order term of the expansion of the free energy for the 3D LG model. The depths decrease with increasing L , and the important question is whether this dip vanishes at T_c or not. Errorbars are omitted but will be reintroduced in Figure 9.

of the dip as a function of system size is shown in Fig. 9. It would clearly have been desirable to be able to access larger system sizes than what we have been able to do in the 3D LG case, to bring out a potential positive curvature that was observed in the 2D CG case. From these results, it is unfortunately not possible to tell whether the depth of the dip remains finite and negative as $L \rightarrow \infty$ or if it vanishes. Hence, we are presently not able to firmly conclude that the inverse dielectric constant in the 3D LG experiences a discontinuity.

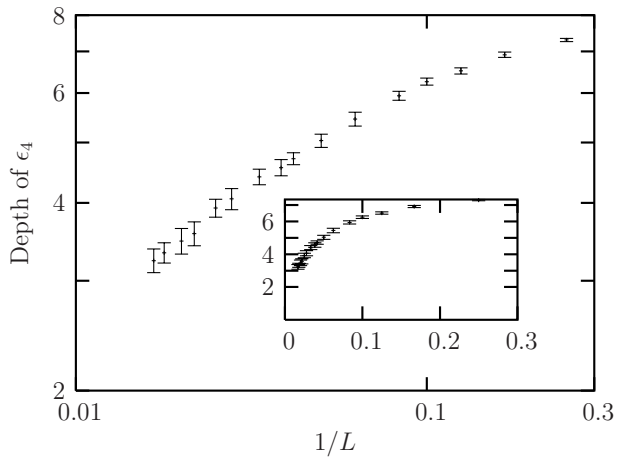


FIG. 9: Depth of the dip in the fourth order term shown in Figure 8 for the 3D LG. The data are obtained from simulations of system sizes ranging from $L = 4$ to $L = 60$ and plotted both on a linear scale (inset) and on a log-log scale. The lack of clear positive curvature in the log-log plot that was observed in 2D CG case makes the extrapolation to the limit $L \rightarrow \infty$ more difficult for the system sizes we have been able to access in 3D.

The temperature locating the minimum in ϵ_4 as a function of system size is shown in Fig. 10 for the 3D LG system. Extrapolation gives $T_c = 0.30 \pm 0.04$.

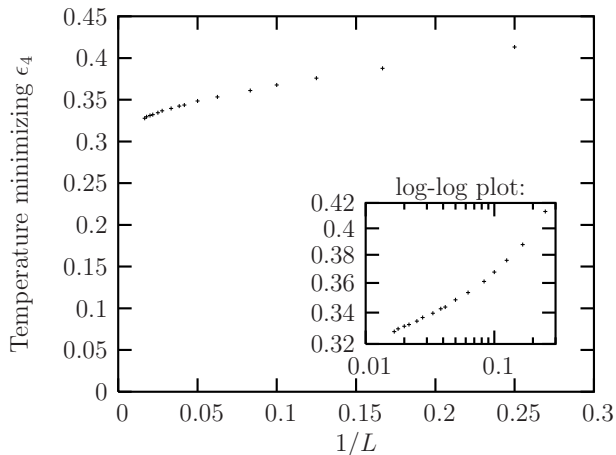


FIG. 10: Temperature minimizing ϵ_4 as a function of inverse system size for the 3D LG system. The values are plotted both on a linear scale and on a log-log scale (inset). This temperature reaches a nonzero value at $L \rightarrow \infty$. Extrapolation gives $T_c = 0.30 \pm 0.04$.

C. 3D Coulomb gas

In this subsection, we contrast the results of the 2D Coulomb gas and the 3D LG to those of the 3D Coulomb gas. The 3D CG is known to be in a metallic high-temperature phase for *all* finite temperatures and should

exhibit quite different finite-size scaling of $\langle s^2 \rangle$ compared to the 2D CG case.^{11,14,25} The results are shown in Fig. 11. Note that the temperature dependence of the curves for all different system sizes are qualitatively different in the 3D CG compared to those in the 2D CG and the 3D LG. This becomes particularly apparent upon considering the L -dependence of $\langle s^2 \rangle$ for various temperatures, where the steepness of the curves increases with decreasing temperature, resulting in a scaling exponent $\alpha(T)$ (from $\langle s^2 \rangle \sim L^{\alpha(T)}$) which decreases with increasing temperature. This is quite consistent with what is known for the 3D CG, namely that it exhibits a metallic state for all finite temperatures, equivalently it corresponds to Polyakov’s permanent confinement.^{11,14} It is evident that the scaling results for $\langle s^2 \rangle$ for the 2D CG and the 3D LG are qualitatively and quantitatively the same, and that they are qualitatively different from those exhibited by the 3D CG. For low temperatures, $\langle s^2 \rangle$ seem to be increasing with temperature. This is only a vacuum effect, since vacuum configurations do not contribute to the measurement of $\langle s^2 \rangle$ ¹⁸. This means that close to vacuum, only configurations resulting from the insertion of one single dipole at the smallest possible distance will contribute. See also section IV D.

The inverse dielectric constant for the 3D CG is shown as a function of temperature in Figure 12 with system sizes ranging up to $L = 50$. Here also, ϵ^{-1} decreases from unity to zero, but the downward drift in the temperature at which ϵ^{-1} deviates from unity seems to be even stronger than for the 3D LG model. Additionally, the decrease towards zero does not sharpen significantly with increasing L .

We find a similar minimum in the fourth order term in the expansion of the free energy for the 3D CG, ϵ_4/L^2 , shown in Fig. 13. However, the dip vanishes as $L \rightarrow \infty$ in the current model. This is clearly shown in Fig. 14 in contrast to the Figs. 4 and 9 of the other two models.

For completeness we have included in Fig. 15 a plot of the temperature locating the minimum in ϵ_4 as a function of system size also for the 3D CG. There is no phase transition to which this temperature is associated, and the stronger downward drift mentioned above is evident when contrasting this plot to Fig. 10 of the 3D LG. The temperature is reduced by a factor 2 in the largest system considered in the 3D CG compared to the smallest whereas the variation is much smaller in the 3D LG. However, there *is* a weak curvature in the log-log version of Fig. 15. Performing a similar extrapolation as we did for the other two models we end up with a “critical” temperature $T_c = 0.24 \pm 0.04$.

D. Charge density

Finally we present in Fig. 16 the charge density for the three models considered. In all three cases the charge densities are independent of L and from these curves we can approximate the average separation r_{mean} between

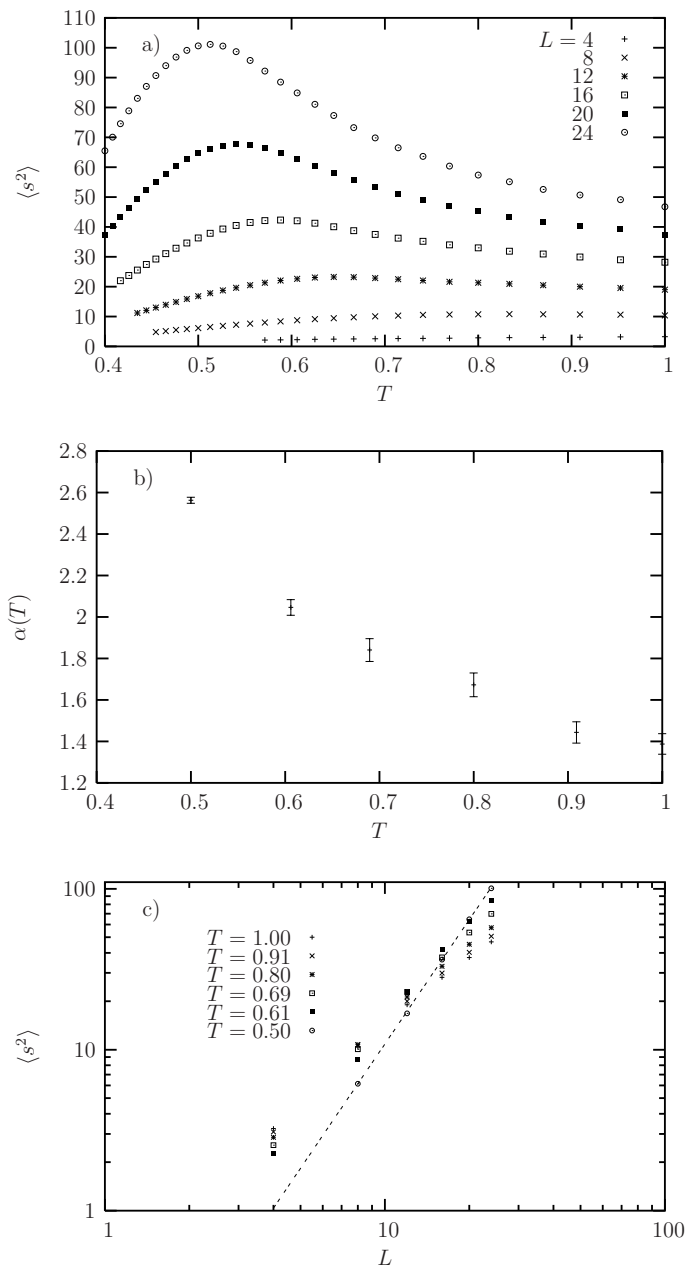


FIG. 11: Mean square dipole moment $\langle s^2 \rangle$ as a function of temperature (top panel) and system size (bottom panel) for the 3D Coulomb gas system of point charges interacting with a $1/r$ bare pair potential. The middle panel shows the scaling exponent α extracted from $\langle s^2 \rangle \sim L^{\alpha(T)}$.

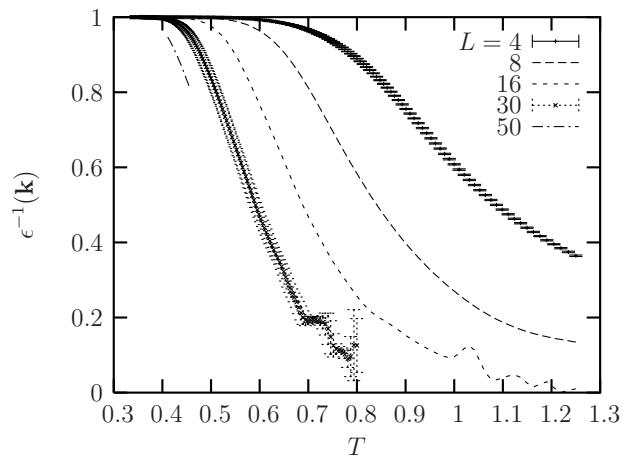


FIG. 12: Inverse dielectric constant taken at the smallest possible wave vector in a finite system, $\mathbf{k} = (0, 2\pi/L, 0)$, and plotted against temperature T for system sizes $L = 4, 8, 16, 30$ and 50 , for the 3D CG system. The decrease of ϵ^{-1} towards zero does not sharpen with increasing L , and there is a clear downward drift in the temperature at which ϵ^{-1} deviates from unity. Errorbars are given in two of the curves, and omitted for clarity in the others.

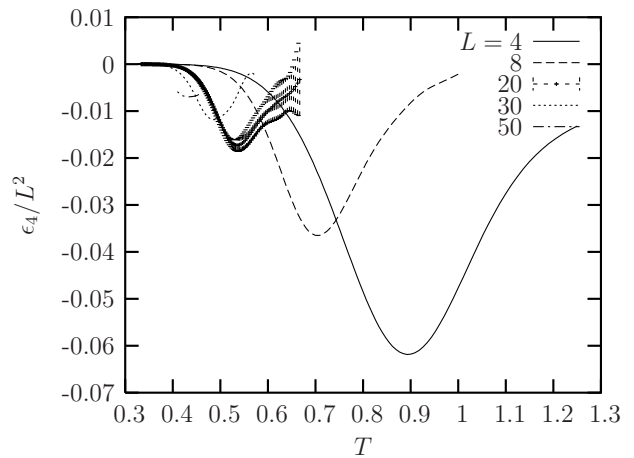


FIG. 13: The coefficient ϵ_4 of the fourth order term of the expansion of the free energy, for the 3D CG. The depths decrease with increasing L and seem to vanish as $L \rightarrow \infty$. Errorbars are shown for one of the systems for demonstration.

the charges assuming uniform distribution,

$$r_{\text{mean}} = \left(\frac{1}{Q_{\text{Sum}}/V} \right)^{1/d}, \quad (12)$$

where d is the dimension. We concentrate on the (L -dependent) temperatures which minimize ϵ_4 . In the two logarithmically interacting models, r_{mean} ranges from ~ 4 for the smallest systems and up to ~ 8 for the largest. In the 3D Coulomb gas on the other hand, r_{mean} remains close to L even for the largest system sizes meaning that the systems are close to their vacuum states at these temperatures. This strongly suggests that the features

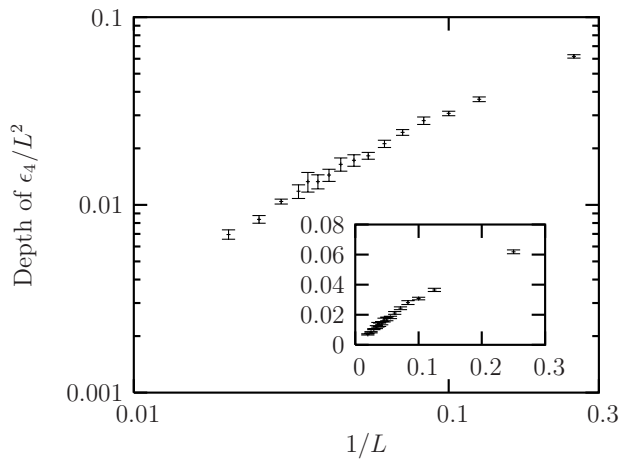


FIG. 14: Depth of the dip in the fourth order term shown in Figure 13 for the 3D CG. The data are obtained from simulations of system sizes ranging from $L = 4$ to $L = 50$ and plotted both on a linear scale (inset) and on a log-log scale. It is clear that the dip vanishes in the thermodynamic limit.

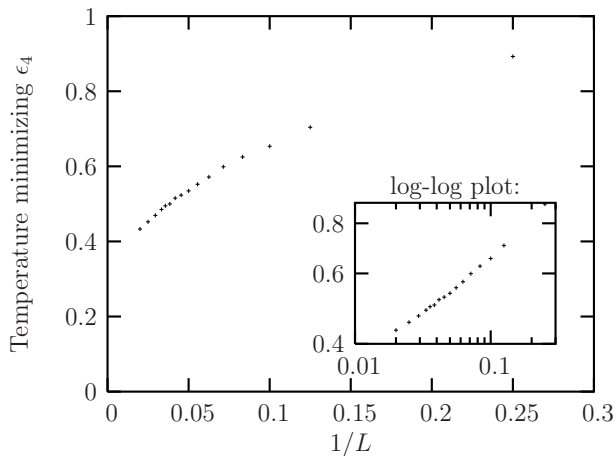


FIG. 15: Temperature minimizing ϵ_4 as a function of inverse system size for the 3D CG system. The values are plotted both on a linear scale and on a log-log scale (inset).

we investigate are only extreme low-density effects in the 3D CG model. Screening, which should take place at all temperatures in a system always being in a metallic state, is not possible in this limit.

In the 2D CG and 3D LG models the situation is different. The interesting temperature domains are smaller and the charge densities are kept close to constant which in turn allows screening for the largest systems.

V. COMMENTS ON UNIVERSALITY

In the 2D CG, the universal jump to zero of the inverse dielectric constant ϵ^{-1} is given by^{19,26}

$$\epsilon^{-1} = \frac{2T_c}{\pi}. \quad (13)$$

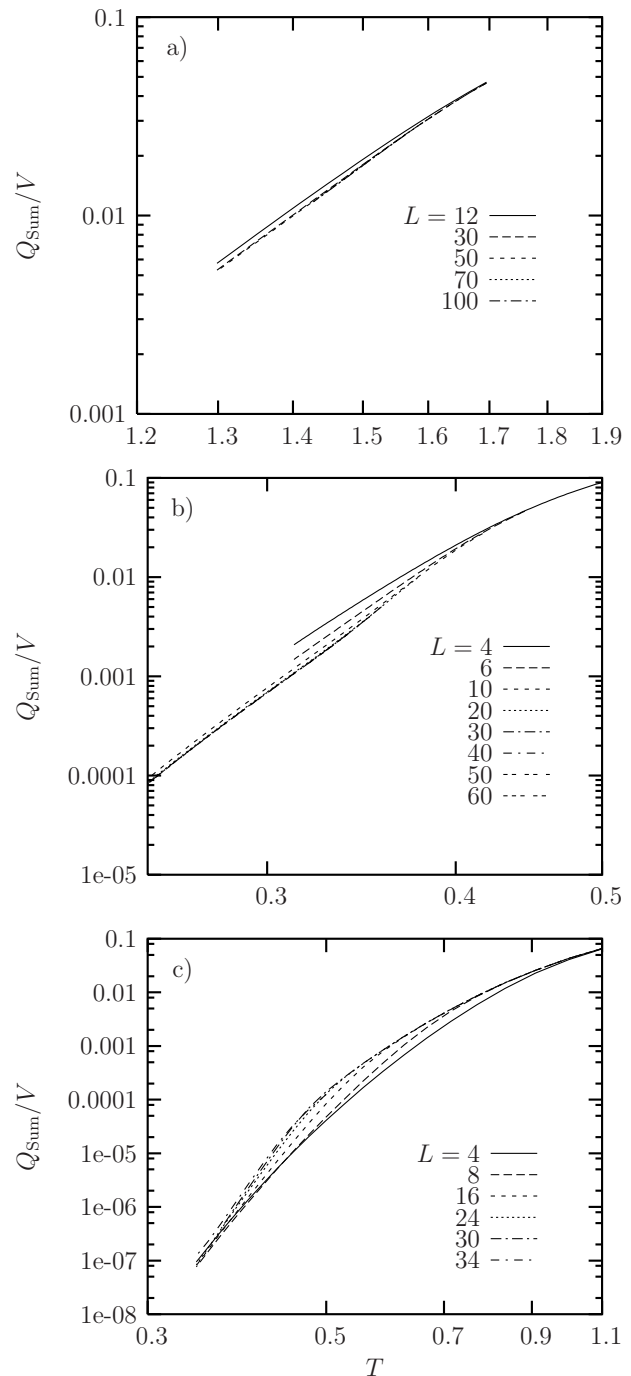


FIG. 16: Charge density Q_{Sum}/V plotted vs. temperature on log-log scales for the a) 2D CG, b) 3D LG and c) 3D CG models. The volume V corresponds to the total number of sites L^d . Note that Q_{Sum}/V is independent of system size L in all three cases.

Using the estimate for the critical temperature found in section IV A, the value at T_c should, according to Eq. (13), be $\epsilon^{-1} = 0.86 \pm 0.03$. This is in agreement with Fig. 2, since it is in this region the curves seem to split.

In Ref. 20, it was speculated that the finite negative value of the fourth order modulus $\langle \Upsilon_4 \rangle \approx -0.130$ could

be associated with a universal number. In the 2D CG, $V_{\mathbf{k}} \sim L^2$ and $Q_{\mathbf{k}}^y \sim 2\pi/L$ for large L , such that the modification $\Delta \rightarrow \Delta/(\sqrt{2}\pi)$ turns (8) into

$$F(\mathbf{T}) - F(0) = \frac{\Delta^2}{2}\epsilon^{-1} + \frac{\Delta^4}{4!}3\epsilon_4. \quad (14)$$

This means that if ϵ^{-1} corresponds to the helicity modulus $\langle \Upsilon \rangle$, it is $3\epsilon_4$ that corresponds to the fourth order modulus $\langle \Upsilon_4 \rangle$. It is interesting to notice that $3\epsilon_4 = -0.141 \pm 0.015$ fits nicely with the value found in Ref. 20, speculated to be a universal number. One may therefore speculate that the value of ϵ_4 at T_c is a universal number independent of T_c . Whether this is a sign of a true universality or a mere coincidence requires further investigation.

One should also note that with this modification of Δ , the additional twist term in the XY-Hamiltonian (1) becomes $\sqrt{2}\Delta \sin(2\pi y/L)/L$. It seems natural to suggest that the net effect of a sine twist is given by its RMS-value, *i.e.* $(1/L \int_0^L \sin^2(2\pi y/L) dy)^{1/2} = 1/\sqrt{2}$. This gives a net twist of Δ across the system, which is the same as in Ref. 20.

The universal jump of ϵ^{-1} in the 3D LG is given by the flow equations derived in Ref. 14. In our units, this jump is predicted to be

$$\epsilon^{-1} = \frac{5T_c}{2}, \quad (15)$$

and by using the critical temperature found in section IV B, this amounts to an ϵ^{-1} in the interval (0.65, 0.85). Since the different curves in Fig. 7 do not merge in the low-temperature regime, as they do in the 2D CG case, it is difficult to make a precise determination of the jump in the 3D LG based on these simulations. However, one can not rule out that the jump lies inside the interval mentioned.

VI. CONCLUDING REMARKS

In this paper we have considered various quantities related to a possible phase transition in systems of point charges interacting with bare logarithmic pair potentials, in 2D and 3D. We have also carried out comparisons with the results obtained in the 3D Coulomb gas in some cases. The quantities we have focused on are the fluctuations of the dipole moment, $\langle s^2 \rangle$, and the fourth order coefficient of the free energy expanded in an appropriate twist. We have shown that the dipole moment fluctuations, associated with the polarizability of the charge systems, has a scaling exponent $\alpha(T)$ defined by $\langle s^2 \rangle \sim L^{\alpha(T)}$ which is positive above some temperature and zero below this temperature for the 2D CG and the 3D LG cases, and is an increasing function of temperature. On the other hand, for the 3D CG case $\alpha(T)$ is finite positive for all temperatures we have considered, and is a *decreasing* function of temperature. This in itself strongly suggests

that the 3D LG has statistical physics much more akin to the 2D CG than to the 3D CG. For the 2D CG we have demonstrated that the inverse dielectric constant experiences a discontinuous jump to zero at the phase transition. This has been done by investigation of a series expansion of free energy using Monte Carlo simulations. The possibility of a universal value of the fourth order term proposed in Ref. 20 has also been commented on, and a possible agreement with this value has been observed. The method developed in this paper will apply to any gas of vortex loops or point charges with any interaction potential. We have applied it to the 3D LG. Although it would have been desirable to be able to access larger system sizes than what we have been able to in the present paper, the results we obtain for the 3D LG suggest that this model may also undergo a metal-insulator transition with a discontinuity in the inverse dielectric function at the critical point, in agreement with the renormalization group results of Ref. 14.

Acknowledgments

This work was supported by the Research Council of Norway, Grant Nos. 158518/431, 158547/431 (NANOMAT), and by the Norwegian High Performance Computing Consortium (NOTUR). One of us (S. K.) acknowledges support from the Norwegian University of Science and Technology. We acknowledge useful discussions with F. S. Nogueira and Z. Tesanovic.

APPENDIX A: DUALITY TRANSFORMATION

The partition function for the XY-model with coupling constant $J = 1$ is

$$Z = \Pi_i \int \frac{d\theta_i}{2\pi} e^{\beta \sum_{\mathbf{r}} \cos(\nabla\theta - 2\pi\mathbf{T})}, \quad (A1)$$

where the sum is over all links between lattice points, $\nabla\theta \equiv \theta_i - \theta_j$ and $\mathbf{T}(\mathbf{r})$ is the twist between the two lattice points sharing the link \mathbf{r} . We will consider three spatial dimensions and comment on any differences in 2D. Applying the Villain approximation, we get

$$Z = \int \mathcal{D}\theta \sum_{\{\mathbf{n}\}} e^{-\frac{\beta}{2} \sum_{\mathbf{r}} (\nabla\theta - 2\pi\mathbf{T} - 2\pi\mathbf{n})^2}. \quad (A2)$$

$\mathbf{n}(\mathbf{r})$ is an integer-valued field taking care of the periodicity of the cosine. By a Hubbard-Stratonovich decoupling, one finds

$$Z = \int \mathcal{D}\theta \mathcal{D}\mathbf{v} \sum_{\{\mathbf{n}\}} e^{-\sum_{\mathbf{r}} [\frac{1}{2\beta} \mathbf{v}^2 + i\mathbf{v} \cdot (\nabla\theta - 2\pi\mathbf{T} - 2\pi\mathbf{n})]}. \quad (A3)$$

The summation over \mathbf{n} may now be evaluated using the Poisson summation formula,

$$\sum_{n=-\infty}^{\infty} e^{2\pi i n v} = \sum_{l=-\infty}^{\infty} \delta(v - l), \quad (A4)$$

at each dual lattice point, yielding

$$Z = \int \mathcal{D}\theta \sum_{\{\mathbf{l}\}} e^{\sum_{\mathbf{r}} 2\pi i \mathbf{l} \cdot \mathbf{T} - i \mathbf{l} \cdot \nabla \theta - \frac{1}{2\beta} \mathbf{l}^2}. \quad (\text{A5})$$

The field $\mathbf{l}(\mathbf{r})$ is integer-valued. Now, performing a partial summation on the second term in the exponent, the θ -integration may be carried out. This produces the constraint that \mathbf{l} must be divergence-free, solved by the introduction of another integer-valued field such that $\mathbf{l} = \nabla \times \mathbf{h}$. Note that $\mathbf{h}(\mathbf{r})$ is a scalar in 2D. The partition function is now

$$Z = \sum_{\{\mathbf{h}\}} e^{\sum_{\mathbf{r}} 2\pi i (\nabla \times \mathbf{h}) \cdot \mathbf{T} - \frac{1}{2\beta} (\nabla \times \mathbf{h})^2}, \quad (\text{A6})$$

and we observe that $\mathbf{h} \rightarrow \mathbf{h} + \nabla \phi$ is a gauge transformation. In two dimensions, the corresponding gauge transformation is $h \rightarrow h + c$, where c is a constant. Using Poisson's summation formula once more, we get

$$Z = \int \mathcal{D}\mathbf{h} \sum_{\{\mathbf{m}\}} e^{\sum_{\mathbf{r}} 2\pi i (\nabla \times \mathbf{h}) \cdot \mathbf{T} - \frac{1}{2\beta} (\nabla \times \mathbf{h})^2 + 2\pi i \mathbf{h} \cdot \mathbf{m}}, \quad (\text{A7})$$

leaving \mathbf{h} no longer integer-valued. The field $\mathbf{m}(\mathbf{r})$ is what corresponds to vortex excitations in the XY model. The gauge invariance of the theory produces the constraint $\sum_{\mathbf{r}} \phi(\nabla \cdot \mathbf{m}) = 0$ for all configurations of \mathbf{m} . Choosing for instance $\phi = \nabla \cdot \mathbf{m}$, it is clear that \mathbf{m} must be divergence-free, *i.e.* the field lines are closed loops. In 2D, the corresponding constraint is $\sum_{\mathbf{r}} m = 0$, indicating an overall charge neutrality in the 2D Coulomb gas or zero total vorticity in the 2D XY model.

By another partial summation, we are now left with a Maxwell term and a coupling term between the gauge field \mathbf{h} and the current $\mathbf{M}(\mathbf{r}) \equiv \mathbf{m} + \nabla \times \mathbf{T}$:

$$Z = \int \mathcal{D}\mathbf{h} \sum_{\{\mathbf{m}\}} e^{\sum_{\mathbf{r}} 2\pi i \mathbf{h} \cdot \mathbf{M} - \frac{1}{2\beta} (\nabla \times \mathbf{h})^2}. \quad (\text{A8})$$

One may now perform a partial integration in the second term and use the gauge where $\nabla \cdot \mathbf{h} = 0$, such that $\nabla \times \nabla \times \mathbf{h} = -\nabla^2 \mathbf{h}$. Then, by going to Fourier space and completing squares, the \mathbf{h} -integration becomes Gaussian. This leaves us with

$$Z = Z_0 \sum_{\{\mathbf{m}\}} e^{\frac{2\beta\pi^2}{N} \sum_{\mathbf{q}} \mathbf{M}_{\mathbf{q}} G_{\mathbf{q}}^{-1} \mathbf{M}_{-\mathbf{q}}}, \quad (\text{A9})$$

where $\nabla^2 e^{\pm i\mathbf{q}\mathbf{r}} \equiv e^{\pm i\mathbf{q}\mathbf{r}} G_{\mathbf{q}}$ and Z_0 is a constant. Defining the discrete Laplacian by

$$\Delta^2 f(\mathbf{r}) = \sum_{\mu} [f(\mathbf{r} + \hat{e}_{\mu}) + f(\mathbf{r} - \hat{e}_{\mu}) - 2f(\mathbf{r})], \quad (\text{A10})$$

it is clear that $G_{\mathbf{q}} = -2 \left(d - \sum_{\mu=1}^d \cos q_{\mu} \right)$, denoting the number of space dimensions by d . Returning to real-space representation, we arrive at

$$Z = Z_0 \sum_{\{\mathbf{m}\}} e^{-\frac{\beta}{2} \sum_{\mathbf{r}_i, \mathbf{r}_j} \mathbf{M}(\mathbf{r}_i) V(|\mathbf{r}_i - \mathbf{r}_j|) \mathbf{M}(\mathbf{r}_j)}, \quad (\text{A11})$$

the interaction being given by

$$V(\mathbf{r}) = \frac{2\pi^2}{L^2} \sum_{\mathbf{q}} \frac{e^{i\mathbf{q}\cdot\mathbf{r}}}{d - \sum_{\mu=1}^d \cos q_{\mu}}. \quad (\text{A12})$$

APPENDIX B: EXPANSION OF FREE ENERGY

Consider the Hamiltonian

$$H_0 = \frac{1}{2} \sum_{i,j} \mathbf{m}_i V_{ij} \mathbf{m}_j, \quad (\text{B1})$$

describing a 3D system of integer-valued currents \mathbf{m} on a lattice interacting via the potential $V_{ij} = V(|\mathbf{r}_i - \mathbf{r}_j|)$. We impose periodic boundary conditions on the system. Perturbing the field \mathbf{m} with a transversal twist turns (B1) into

$$H = \frac{1}{2} \sum_{i,j} (\mathbf{m} + \nabla \times \mathbf{T})_i V_{ij} (\mathbf{m} + \nabla \times \mathbf{T})_j. \quad (\text{B2})$$

We let the linear system size be L and define the discrete Fourier transform by

$$f_{\mathbf{q}} = \sum_{\mathbf{r}} f(\mathbf{r}) e^{i\mathbf{q}\cdot\mathbf{r}}, \quad (\text{B3})$$

where $\mathbf{r} = (n_x, n_y, n_z)$ and $n_i = 0, \dots, L-1$. The inverse transform is

$$f(\mathbf{r}) = \frac{1}{N} \sum_{\mathbf{q}} f_{\mathbf{q}} e^{-i\mathbf{q}\cdot\mathbf{r}}, \quad (\text{B4})$$

where $\mathbf{q} = \frac{2\pi}{L}(k_x, k_y, k_z)$ and $k_i = -L/2 + 1, \dots, L/2$. N is the number of lattice sites. Let us also define $Q_{\pm\mathbf{q}}^{\nu}$ by $\Delta^{\nu} e^{\pm i\mathbf{q}\cdot\mathbf{r}} = e^{\pm i\mathbf{q}\cdot\mathbf{r}} Q_{\pm\mathbf{q}}^{\nu}$, where Δ^{ν} is a lattice derivative. In Fourier representation the Hamiltonian becomes

$$H = \frac{1}{2N} \sum_{\mathbf{q}} (m_{\mathbf{q}}^{\mu} + \varepsilon^{\mu\nu\lambda} Q_{-\mathbf{q}}^{\nu} T_{\mathbf{q}}^{\lambda}) V_{\mathbf{q}} (m_{-\mathbf{q}}^{\mu} + \varepsilon^{\mu\rho\sigma} Q_{\mathbf{q}}^{\rho} T_{-\mathbf{q}}^{\sigma}). \quad (\text{B5})$$

For later use, we calculate the derivative of H , which is

$$\frac{\partial H}{\partial T_{\mathbf{q}_1}^{\alpha}} = \frac{1}{N} \varepsilon^{\mu\nu\alpha} Q_{-\mathbf{q}_1}^{\nu} (m_{-\mathbf{q}_1}^{\mu} + \varepsilon^{\mu\rho\sigma} Q_{\mathbf{q}_1}^{\rho} T_{-\mathbf{q}_1}^{\sigma}) V_{\mathbf{q}_1}. \quad (\text{B6})$$

We also note that

$$\frac{\partial^2 H}{\partial T_{\mathbf{q}_1}^{\alpha} \partial T_{\mathbf{q}_2}^{\beta}} = \frac{1}{N} \varepsilon^{\mu\nu\alpha} \varepsilon^{\mu\rho\beta} Q_{-\mathbf{q}_1}^{\nu} Q_{\mathbf{q}_1}^{\rho} V_{\mathbf{q}_1} \delta_{\mathbf{q}_1 + \mathbf{q}_2, 0} \quad (\text{B7})$$

is independent of \mathbf{m} and that all higher order derivatives are zero.

The free energy is given by $F = -T \ln Z$, where the partition function is

$$Z = \sum_{\{\mathbf{m}\}} e^{-H/T}, \quad (\text{B8})$$

summing over all possible configurations of \mathbf{m} . By Taylor expansion of the free energy in the twist, we get

$$F(\mathbf{T}) - F(0) = \sum_{\alpha} \sum_{\mathbf{r}_1} \left. \frac{\partial F}{\partial T^{\alpha}(\mathbf{r}_1)} \right|_{\mathbf{T}=0} T^{\alpha}(\mathbf{r}_1) + \sum_{\alpha, \beta} \sum_{\mathbf{r}_1, \mathbf{r}_2} \left. \frac{\partial^2 F}{\partial T^{\alpha}(\mathbf{r}_1) \partial T^{\beta}(\mathbf{r}_2)} \right|_{\mathbf{T}=0} T^{\alpha}(\mathbf{r}_1) T^{\beta}(\mathbf{r}_2) + \dots \quad (\text{B9})$$

Note that $F(\mathbf{T} = 0)$ refers to the free energy of the unperturbed system described by H_0 . By writing each term in the series in Fourier representation, one finds the equivalent expansion in Fourier components of the twist, *i.e.*

$$F(\mathbf{T}) - F(0) = \sum_{\alpha} \sum_{\mathbf{q}_1} \left. \frac{\partial F}{\partial T_{\mathbf{q}_1}^{\alpha}} \right|_{\mathbf{T}=0} T_{\mathbf{q}_1}^{\alpha} + \sum_{\alpha, \beta} \sum_{\mathbf{q}_1, \mathbf{q}_2} \left. \frac{\partial^2 F}{\partial T_{\mathbf{q}_1}^{\alpha} \partial T_{\mathbf{q}_2}^{\beta}} \right|_{\mathbf{T}=0} \frac{T_{\mathbf{q}_1}^{\alpha} T_{\mathbf{q}_2}^{\beta}}{2} + \dots \quad (\text{B10})$$

The first derivative becomes

$$\frac{\partial F}{\partial T_{\mathbf{q}_1}^{\alpha}} = \frac{1}{Z} \sum_{\{\mathbf{m}\}} \frac{\partial H}{\partial T_{\mathbf{q}_1}^{\alpha}} e^{-H/T} \equiv \left\langle \frac{\partial H}{\partial T_{\mathbf{q}_1}^{\alpha}} \right\rangle. \quad (\text{B11})$$

Proceeding, we find

$$\frac{\partial^2 F}{\partial T_{\mathbf{q}_1}^{\alpha} \partial T_{\mathbf{q}_2}^{\beta}} = \frac{1}{T} \left\langle \frac{\partial H}{\partial T_{\mathbf{q}_1}^{\alpha}} \right\rangle \left\langle \frac{\partial H}{\partial T_{\mathbf{q}_2}^{\beta}} \right\rangle + \frac{\partial^2 H}{\partial T_{\mathbf{q}_1}^{\alpha} \partial T_{\mathbf{q}_2}^{\beta}} - \frac{1}{T} \left\langle \frac{\partial H}{\partial T_{\mathbf{q}_1}^{\alpha}} \frac{\partial H}{\partial T_{\mathbf{q}_2}^{\beta}} \right\rangle \quad (\text{B12})$$

for the second derivative and

$$\begin{aligned} \frac{\partial^3 F}{\partial T_{\mathbf{q}_1}^{\alpha} \partial T_{\mathbf{q}_2}^{\beta} \partial T_{\mathbf{q}_3}^{\gamma}} &= \frac{1}{T^2} \left[2 \left\langle \frac{\partial H}{\partial T_{\mathbf{q}_1}^{\alpha}} \right\rangle \left\langle \frac{\partial H}{\partial T_{\mathbf{q}_2}^{\beta}} \right\rangle \left\langle \frac{\partial H}{\partial T_{\mathbf{q}_3}^{\gamma}} \right\rangle + \left\langle \frac{\partial H}{\partial T_{\mathbf{q}_1}^{\alpha}} \frac{\partial H}{\partial T_{\mathbf{q}_2}^{\beta}} \frac{\partial H}{\partial T_{\mathbf{q}_3}^{\gamma}} \right\rangle \right. \\ &\quad - \left\langle \frac{\partial H}{\partial T_{\mathbf{q}_1}^{\alpha}} \right\rangle \left\langle \frac{\partial H}{\partial T_{\mathbf{q}_2}^{\beta}} \frac{\partial H}{\partial T_{\mathbf{q}_3}^{\gamma}} \right\rangle - \left\langle \frac{\partial H}{\partial T_{\mathbf{q}_2}^{\beta}} \right\rangle \left\langle \frac{\partial H}{\partial T_{\mathbf{q}_1}^{\alpha}} \frac{\partial H}{\partial T_{\mathbf{q}_3}^{\gamma}} \right\rangle \\ &\quad \left. - \left\langle \frac{\partial H}{\partial T_{\mathbf{q}_3}^{\gamma}} \right\rangle \left\langle \frac{\partial H}{\partial T_{\mathbf{q}_1}^{\alpha}} \frac{\partial H}{\partial T_{\mathbf{q}_2}^{\beta}} \right\rangle \right] \quad (\text{B13}) \end{aligned}$$

for the third. We have exploited the fact that third derivatives of H vanishes. The fourth derivative is found to be

$$\begin{aligned}
\frac{\partial^4 F}{\partial T_{\mathbf{q}_1}^\alpha \partial T_{\mathbf{q}_2}^\beta \partial T_{\mathbf{q}_3}^\gamma \partial T_{\mathbf{q}_4}^\delta} &= \frac{1}{T^3} \left\{ 6 \left\langle \frac{\partial H}{\partial T_{\mathbf{q}_1}^\alpha} \right\rangle \left\langle \frac{\partial H}{\partial T_{\mathbf{q}_2}^\beta} \right\rangle \left\langle \frac{\partial H}{\partial T_{\mathbf{q}_3}^\gamma} \right\rangle \left\langle \frac{\partial H}{\partial T_{\mathbf{q}_4}^\delta} \right\rangle \right. \\
&\quad - 2 \left[\left\langle \frac{\partial H}{\partial T_{\mathbf{q}_1}^\alpha} \right\rangle \left\langle \frac{\partial H}{\partial T_{\mathbf{q}_2}^\beta} \right\rangle \left\langle \frac{\partial H}{\partial T_{\mathbf{q}_3}^\gamma} \frac{\partial H}{\partial T_{\mathbf{q}_4}^\delta} \right\rangle + \left\langle \frac{\partial H}{\partial T_{\mathbf{q}_1}^\alpha} \right\rangle \left\langle \frac{\partial H}{\partial T_{\mathbf{q}_3}^\gamma} \right\rangle \left\langle \frac{\partial H}{\partial T_{\mathbf{q}_2}^\beta} \frac{\partial H}{\partial T_{\mathbf{q}_4}^\delta} \right\rangle \right. \\
&\quad + \left\langle \frac{\partial H}{\partial T_{\mathbf{q}_1}^\alpha} \right\rangle \left\langle \frac{\partial H}{\partial T_{\mathbf{q}_4}^\delta} \right\rangle \left\langle \frac{\partial H}{\partial T_{\mathbf{q}_2}^\beta} \frac{\partial H}{\partial T_{\mathbf{q}_3}^\gamma} \right\rangle + \left\langle \frac{\partial H}{\partial T_{\mathbf{q}_2}^\beta} \right\rangle \left\langle \frac{\partial H}{\partial T_{\mathbf{q}_3}^\gamma} \right\rangle \left\langle \frac{\partial H}{\partial T_{\mathbf{q}_1}^\alpha} \frac{\partial H}{\partial T_{\mathbf{q}_4}^\delta} \right\rangle \\
&\quad + \left\langle \frac{\partial H}{\partial T_{\mathbf{q}_2}^\beta} \right\rangle \left\langle \frac{\partial H}{\partial T_{\mathbf{q}_4}^\delta} \right\rangle \left\langle \frac{\partial H}{\partial T_{\mathbf{q}_1}^\alpha} \frac{\partial H}{\partial T_{\mathbf{q}_3}^\gamma} \right\rangle + \left. \left\langle \frac{\partial H}{\partial T_{\mathbf{q}_3}^\gamma} \right\rangle \left\langle \frac{\partial H}{\partial T_{\mathbf{q}_4}^\delta} \right\rangle \left\langle \frac{\partial H}{\partial T_{\mathbf{q}_1}^\alpha} \frac{\partial H}{\partial T_{\mathbf{q}_2}^\beta} \right\rangle \right] \\
&\quad + \left\langle \frac{\partial H}{\partial T_{\mathbf{q}_1}^\alpha} \right\rangle \left\langle \frac{\partial H}{\partial T_{\mathbf{q}_2}^\beta} \frac{\partial H}{\partial T_{\mathbf{q}_3}^\gamma} \frac{\partial H}{\partial T_{\mathbf{q}_4}^\delta} \right\rangle + \left\langle \frac{\partial H}{\partial T_{\mathbf{q}_2}^\beta} \right\rangle \left\langle \frac{\partial H}{\partial T_{\mathbf{q}_1}^\alpha} \frac{\partial H}{\partial T_{\mathbf{q}_3}^\gamma} \frac{\partial H}{\partial T_{\mathbf{q}_4}^\delta} \right\rangle \\
&\quad + \left\langle \frac{\partial H}{\partial T_{\mathbf{q}_3}^\gamma} \right\rangle \left\langle \frac{\partial H}{\partial T_{\mathbf{q}_1}^\alpha} \frac{\partial H}{\partial T_{\mathbf{q}_2}^\beta} \frac{\partial H}{\partial T_{\mathbf{q}_4}^\delta} \right\rangle + \left\langle \frac{\partial H}{\partial T_{\mathbf{q}_4}^\delta} \right\rangle \left\langle \frac{\partial H}{\partial T_{\mathbf{q}_1}^\alpha} \frac{\partial H}{\partial T_{\mathbf{q}_2}^\beta} \frac{\partial H}{\partial T_{\mathbf{q}_3}^\gamma} \right\rangle \\
&\quad + \left\langle \frac{\partial H}{\partial T_{\mathbf{q}_1}^\alpha} \frac{\partial H}{\partial T_{\mathbf{q}_2}^\beta} \right\rangle \left\langle \frac{\partial H}{\partial T_{\mathbf{q}_3}^\gamma} \frac{\partial H}{\partial T_{\mathbf{q}_4}^\delta} \right\rangle + \left\langle \frac{\partial H}{\partial T_{\mathbf{q}_1}^\alpha} \frac{\partial H}{\partial T_{\mathbf{q}_3}^\gamma} \right\rangle \left\langle \frac{\partial H}{\partial T_{\mathbf{q}_2}^\beta} \frac{\partial H}{\partial T_{\mathbf{q}_4}^\delta} \right\rangle \\
&\quad + \left. \left\langle \frac{\partial H}{\partial T_{\mathbf{q}_1}^\alpha} \frac{\partial H}{\partial T_{\mathbf{q}_4}^\delta} \right\rangle \left\langle \frac{\partial H}{\partial T_{\mathbf{q}_2}^\beta} \frac{\partial H}{\partial T_{\mathbf{q}_3}^\gamma} \right\rangle - \left\langle \frac{\partial H}{\partial T_{\mathbf{q}_1}^\alpha} \frac{\partial H}{\partial T_{\mathbf{q}_2}^\beta} \frac{\partial H}{\partial T_{\mathbf{q}_3}^\gamma} \frac{\partial H}{\partial T_{\mathbf{q}_4}^\delta} \right\rangle \right\}.
\end{aligned} \tag{B14}$$

Remembering that

$$\left. \frac{\partial H}{\partial T_{\mathbf{q}_1}^\alpha} \right|_{\mathbf{T}=0} = \frac{1}{N} \varepsilon^{\mu\nu\alpha} Q_{-\mathbf{q}_1}^\nu m_{-\mathbf{q}_1}^\mu V_{\mathbf{q}_1}, \tag{B15}$$

it is straightforward to write the derivatives at zero twist as \mathbf{m} -correlators. However, in many cases these expressions may be simplified further. If the sum over all possible configurations $\{\mathbf{m}\}$ is symmetric around zero, one finds that all odd-order correlators are zero, resulting in

$$\left. \frac{\partial F}{\partial T_{\mathbf{q}_1}^\alpha} \right|_{\mathbf{T}=0} = \left. \frac{\partial^3 F}{\partial T_{\mathbf{q}_1}^\alpha \partial T_{\mathbf{q}_2}^\beta \partial T_{\mathbf{q}_3}^\gamma} \right|_{\mathbf{T}=0} = 0. \tag{B16}$$

Furthermore, since $V_{ij} = V(|\mathbf{r}_i - \mathbf{r}_j|)$, *i.e.* we have a translationally invariant system, the even-order correlators are subject to relations like

$$\langle m_{-\mathbf{q}_1}^\mu m_{-\mathbf{q}_2}^\nu \rangle = \langle m_{-\mathbf{q}_1}^\mu m_{-\mathbf{q}_2}^\nu \rangle \delta_{\mathbf{q}_1 + \mathbf{q}_2, 0} \tag{B17}$$

and

$$\langle m_{-\mathbf{q}_1}^\mu m_{-\mathbf{q}_2}^\nu m_{-\mathbf{q}_3}^\kappa m_{-\mathbf{q}_4}^\lambda \rangle = \langle m_{-\mathbf{q}_1}^\mu m_{-\mathbf{q}_2}^\nu m_{-\mathbf{q}_3}^\kappa m_{-\mathbf{q}_4}^\lambda \rangle \delta_{\mathbf{q}_1 + \mathbf{q}_2 + \mathbf{q}_3 + \mathbf{q}_4, 0}. \tag{B18}$$

Thus, we find

$$\left. \frac{\partial^2 F}{\partial T_{\mathbf{q}_1}^\alpha \partial T_{\mathbf{q}_2}^\beta} \right|_{\mathbf{T}=0} = \frac{\varepsilon^{\mu\sigma\alpha} \varepsilon^{\nu\rho\beta} Q_{-\mathbf{q}_1}^\sigma Q_{-\mathbf{q}_2}^\rho V_{\mathbf{q}_1} \delta_{\mathbf{q}_1 + \mathbf{q}_2, 0}}{N} \left(\delta^{\mu\nu} - \frac{V_{\mathbf{q}_2}}{NT} \langle m_{-\mathbf{q}_1}^\mu m_{-\mathbf{q}_2}^\nu \rangle \right) \tag{B19}$$

for the second derivative and

$$\begin{aligned}
\left. \frac{\partial^4 F}{\partial T_{\mathbf{q}_1}^\alpha \partial T_{\mathbf{q}_2}^\beta \partial T_{\mathbf{q}_3}^\gamma \partial T_{\mathbf{q}_4}^\delta} \right|_{\mathbf{T}=0} &= \frac{\varepsilon^{\mu\sigma\alpha} \varepsilon^{\nu\rho\beta} \varepsilon^{\kappa\tau\gamma} \varepsilon^{\lambda\eta\delta} Q_{-\mathbf{q}_1}^\sigma Q_{-\mathbf{q}_2}^\rho Q_{-\mathbf{q}_3}^\tau Q_{-\mathbf{q}_4}^\eta V_{\mathbf{q}_1} V_{\mathbf{q}_2} V_{\mathbf{q}_3} V_{\mathbf{q}_4}}{N^4 T^3} \\
&\quad \times \left\{ \langle m_{-\mathbf{q}_1}^\mu m_{-\mathbf{q}_2}^\nu \rangle \langle m_{-\mathbf{q}_3}^\kappa m_{-\mathbf{q}_4}^\lambda \rangle \delta_{\mathbf{q}_1 + \mathbf{q}_2, 0} \delta_{\mathbf{q}_3 + \mathbf{q}_4, 0} \right. \\
&\quad + \langle m_{-\mathbf{q}_1}^\mu m_{-\mathbf{q}_3}^\kappa \rangle \langle m_{-\mathbf{q}_2}^\nu m_{-\mathbf{q}_4}^\lambda \rangle \delta_{\mathbf{q}_1 + \mathbf{q}_3, 0} \delta_{\mathbf{q}_2 + \mathbf{q}_4, 0} \\
&\quad + \langle m_{-\mathbf{q}_1}^\mu m_{-\mathbf{q}_4}^\lambda \rangle \langle m_{-\mathbf{q}_2}^\nu m_{-\mathbf{q}_3}^\kappa \rangle \delta_{\mathbf{q}_1 + \mathbf{q}_4, 0} \delta_{\mathbf{q}_2 + \mathbf{q}_3, 0} \\
&\quad \left. - \langle m_{-\mathbf{q}_1}^\mu m_{-\mathbf{q}_2}^\nu m_{-\mathbf{q}_3}^\kappa m_{-\mathbf{q}_4}^\lambda \rangle \delta_{\mathbf{q}_1 + \mathbf{q}_2 + \mathbf{q}_3 + \mathbf{q}_4, 0} \right\}
\end{aligned} \tag{B20}$$

for the fourth. These expressions may also be applied to a gas of point charges in 2D or 3D, that is when m is a scalar field. One way to do this is by replacing $\nabla \times \mathbf{T}$ in (B2) with its z -component $\varepsilon^{z\nu\lambda}\Delta^\nu T^\lambda$, with the consequence that the greek letter summations may be taken over x and y only. For the second derivative, this results in

$$\left. \frac{\partial^2 F}{\partial T_{\mathbf{q}_1}^\alpha \partial T_{\mathbf{q}_2}^\beta} \right|_{\mathbf{T}=0} = \frac{\varepsilon^{z\sigma\alpha}\varepsilon^{z\rho\beta} Q_{-\mathbf{q}_1}^\sigma Q_{\mathbf{q}_1}^\rho V_{\mathbf{q}_1} \delta_{\mathbf{q}_1+\mathbf{q}_2,0}}{N} \left(1 - \frac{V_{\mathbf{q}_1}}{NT} \langle m_{\mathbf{q}_1} m_{-\mathbf{q}_1} \rangle \right), \quad (\text{B21})$$

where we have applied $V_{\mathbf{q}} = V_{-\mathbf{q}}$. We recognize the paranthesis as the Fourier transform of the inverse dielectric response function $\varepsilon^{-1}(\mathbf{q}_1)$ in the low density limit. Note that the factor

$$\varepsilon^{z\sigma\alpha}\varepsilon^{z\rho\beta} Q_{-\mathbf{q}_1}^\sigma Q_{\mathbf{q}_1}^\rho = Q_{\mathbf{q}_1}^\sigma Q_{-\mathbf{q}_1}^\rho \left(1 - \frac{Q_{\mathbf{q}_1}^\alpha Q_{-\mathbf{q}_1}^\beta}{Q_{\mathbf{q}_1}^\sigma Q_{-\mathbf{q}_1}^\rho} \right) \quad (\text{B22})$$

is a projection operator times $Q_{\mathbf{q}_1}^\sigma Q_{-\mathbf{q}_1}^\rho \sim q_{1x}^2 + q_{1y}^2$, reflecting the transversality of the twist.

To arrive at eq. (8), we chose the twist (7) and computed the sums appearing in the expansion (B10) for both the second and fourth order term. The sum over direction is trivial, since our twist points in the x -direction. The sum over momenta is also managable, since $T_{\mathbf{q}}^x$ has nonzero values only for $\mathbf{q} = (0, \pm 2\pi/L)$. This sum gives two contributions in the second order term, due to the restriction $\delta_{\mathbf{q}_1+\mathbf{q}_2,0}$. The same argument results in four contributions for the three terms in (B20) being a product of two second order correlators. The term containing a fourth order correlator will give six contributions due

to the restriction $\delta_{\mathbf{q}_1+\mathbf{q}_2+\mathbf{q}_3+\mathbf{q}_4,0}$.

APPENDIX C: HIGHER ORDER TERMS

Using the method described in this paper involves extrapolation to $L \rightarrow \infty$ and deciding whether or not the fourth order term in the expansion (B10) goes to zero or to a finite nonzero value. This procedure could in some cases be difficult. However, if the fourth order term had turned out to be zero in the thermodynamic limit, it would *not* necessarily mean that the second order term, the inverse dielectric response function, would have to go continuously to zero. In fact, if one were able to prove that the fourth order term is negative *or* zero, one could go on to investigate the sixth order term instead. If it then turned out that the value of the sixth order term was hard to establish, one could in principle repeat the procedure and go to higher order terms. We therefore include the sixth derivative here. To simplify calculations, we work with a twist in the x -direction only.

$$\begin{aligned} & \overline{\frac{\partial^6 F}{\partial T_{\mathbf{q}_1}^x \partial T_{\mathbf{q}_2}^x \partial T_{\mathbf{q}_3}^x \partial T_{\mathbf{q}_4}^x \partial T_{\mathbf{q}_5}^x \partial T_{\mathbf{q}_6}^x}} = \\ & \frac{1}{T^5} \left\{ 120 \left\langle \frac{\partial H}{\partial T_{\mathbf{q}_1}^x} \right\rangle \left\langle \frac{\partial H}{\partial T_{\mathbf{q}_2}^x} \right\rangle \left\langle \frac{\partial H}{\partial T_{\mathbf{q}_3}^x} \right\rangle \left\langle \frac{\partial H}{\partial T_{\mathbf{q}_4}^x} \right\rangle \left[\left\langle \frac{\partial H}{\partial T_{\mathbf{q}_5}^x} \right\rangle \left\langle \frac{\partial H}{\partial T_{\mathbf{q}_6}^x} \right\rangle - 3 \left\langle \frac{\partial H}{\partial T_{\mathbf{q}_5}^x} \frac{\partial H}{\partial T_{\mathbf{q}_6}^x} \right\rangle \right] \right. \\ & + 18 \left\langle \frac{\partial H}{\partial T_{\mathbf{q}_1}^x} \frac{\partial H}{\partial T_{\mathbf{q}_2}^x} \right\rangle \left[13 \left\langle \frac{\partial H}{\partial T_{\mathbf{q}_3}^x} \right\rangle \left\langle \frac{\partial H}{\partial T_{\mathbf{q}_4}^x} \right\rangle \left\langle \frac{\partial H}{\partial T_{\mathbf{q}_5}^x} \frac{\partial H}{\partial T_{\mathbf{q}_6}^x} \right\rangle - \left\langle \frac{\partial H}{\partial T_{\mathbf{q}_3}^x} \frac{\partial H}{\partial T_{\mathbf{q}_4}^x} \right\rangle \left\langle \frac{\partial H}{\partial T_{\mathbf{q}_5}^x} \frac{\partial H}{\partial T_{\mathbf{q}_6}^x} \right\rangle \right] \\ & + 2 \left\langle \frac{\partial H}{\partial T_{\mathbf{q}_1}^x} \frac{\partial H}{\partial T_{\mathbf{q}_2}^x} \frac{\partial H}{\partial T_{\mathbf{q}_3}^x} \right\rangle \left[5 \left\langle \frac{\partial H}{\partial T_{\mathbf{q}_4}^x} \frac{\partial H}{\partial T_{\mathbf{q}_5}^x} \frac{\partial H}{\partial T_{\mathbf{q}_6}^x} \right\rangle - 48 \left\langle \frac{\partial H}{\partial T_{\mathbf{q}_4}^x} \right\rangle \left\langle \frac{\partial H}{\partial T_{\mathbf{q}_5}^x} \frac{\partial H}{\partial T_{\mathbf{q}_6}^x} \right\rangle + 60 \left\langle \frac{\partial H}{\partial T_{\mathbf{q}_4}^x} \right\rangle \left\langle \frac{\partial H}{\partial T_{\mathbf{q}_5}^x} \right\rangle \left\langle \frac{\partial H}{\partial T_{\mathbf{q}_6}^x} \right\rangle \right] \\ & + 15 \left\langle \frac{\partial H}{\partial T_{\mathbf{q}_1}^x} \frac{\partial H}{\partial T_{\mathbf{q}_2}^x} \frac{\partial H}{\partial T_{\mathbf{q}_3}^x} \frac{\partial H}{\partial T_{\mathbf{q}_4}^x} \right\rangle \left[\left\langle \frac{\partial H}{\partial T_{\mathbf{q}_5}^x} \frac{\partial H}{\partial T_{\mathbf{q}_6}^x} \right\rangle - 2 \left\langle \frac{\partial H}{\partial T_{\mathbf{q}_5}^x} \right\rangle \left\langle \frac{\partial H}{\partial T_{\mathbf{q}_6}^x} \right\rangle \right] \\ & + 6 \left\langle \frac{\partial H}{\partial T_{\mathbf{q}_1}^x} \right\rangle \left\langle \frac{\partial H}{\partial T_{\mathbf{q}_2}^x} \frac{\partial H}{\partial T_{\mathbf{q}_3}^x} \frac{\partial H}{\partial T_{\mathbf{q}_4}^x} \frac{\partial H}{\partial T_{\mathbf{q}_5}^x} \frac{\partial H}{\partial T_{\mathbf{q}_6}^x} \right\rangle - \left\langle \frac{\partial H}{\partial T_{\mathbf{q}_1}^x} \frac{\partial H}{\partial T_{\mathbf{q}_2}^x} \frac{\partial H}{\partial T_{\mathbf{q}_3}^x} \frac{\partial H}{\partial T_{\mathbf{q}_4}^x} \frac{\partial H}{\partial T_{\mathbf{q}_5}^x} \frac{\partial H}{\partial T_{\mathbf{q}_6}^x} \right\rangle \left. \right\} \\ & - \frac{12}{T^4} \frac{\partial^2 H}{\partial T_{\mathbf{q}_1}^x \partial T_{\mathbf{q}_2}^x} \left\{ 2 \left\langle \frac{\partial H}{\partial T_{\mathbf{q}_3}^x} \right\rangle \left\langle \frac{\partial H}{\partial T_{\mathbf{q}_4}^x} \right\rangle \left\langle \frac{\partial H}{\partial T_{\mathbf{q}_5}^x} \frac{\partial H}{\partial T_{\mathbf{q}_6}^x} \right\rangle + 2 \left\langle \frac{\partial H}{\partial T_{\mathbf{q}_3}^x} \frac{\partial H}{\partial T_{\mathbf{q}_4}^x} \right\rangle \left\langle \frac{\partial H}{\partial T_{\mathbf{q}_5}^x} \frac{\partial H}{\partial T_{\mathbf{q}_6}^x} \right\rangle \right. \\ & \left. + \left\langle \frac{\partial H}{\partial T_{\mathbf{q}_3}^x} \right\rangle \left\langle \frac{\partial H}{\partial T_{\mathbf{q}_4}^x} \frac{\partial H}{\partial T_{\mathbf{q}_5}^x} \frac{\partial H}{\partial T_{\mathbf{q}_6}^x} \right\rangle \right\} + \frac{12}{T^3} \frac{\partial^2 H}{\partial T_{\mathbf{q}_1}^x \partial T_{\mathbf{q}_2}^x} \frac{\partial^2 H}{\partial T_{\mathbf{q}_3}^x \partial T_{\mathbf{q}_4}^x} \left\{ \left\langle \frac{\partial H}{\partial T_{\mathbf{q}_5}^x} \frac{\partial H}{\partial T_{\mathbf{q}_6}^x} \right\rangle + 2 \left\langle \frac{\partial H}{\partial T_{\mathbf{q}_5}^x} \right\rangle \left\langle \frac{\partial H}{\partial T_{\mathbf{q}_6}^x} \right\rangle \right\}. \end{aligned} \quad (\text{C1})$$

Note that we are allowed to permute the momenta $\mathbf{q}_1, \dots, \mathbf{q}_6$, since these are summed over in the free energy expansion. Assuming vanishing odd-order correlators and imposing that m is a scalar field gives

$$\begin{aligned} \frac{\partial^6 F}{\partial T_{\mathbf{q}_1}^x \partial T_{\mathbf{q}_2}^x \partial T_{\mathbf{q}_3}^x \partial T_{\mathbf{q}_4}^x \partial T_{\mathbf{q}_5}^x \partial T_{\mathbf{q}_6}^x} &= \frac{Q_{-\mathbf{q}_1}^y Q_{-\mathbf{q}_2}^y Q_{-\mathbf{q}_3}^y Q_{-\mathbf{q}_4}^y Q_{-\mathbf{q}_5}^y Q_{-\mathbf{q}_6}^y V_{\mathbf{q}_1} V_{\mathbf{q}_2} V_{\mathbf{q}_3} V_{\mathbf{q}_4}}{N^4 T^3} \\ &\times \left\{ 12 \langle m_{-\mathbf{q}_1} m_{-\mathbf{q}_2} \rangle \left[1 - \frac{2V_{\mathbf{q}_5}}{NT} \langle m_{-\mathbf{q}_3} m_{-\mathbf{q}_4} \rangle \right] \delta_{\mathbf{q}_1+\mathbf{q}_2,0} \delta_{\mathbf{q}_3+\mathbf{q}_4,0} \delta_{\mathbf{q}_5+\mathbf{q}_6,0} \right. \\ &\quad - \frac{V_{\mathbf{q}_5} V_{\mathbf{q}_6}}{N^2 T^2} \left[\langle m_{-\mathbf{q}_1} m_{-\mathbf{q}_2} m_{-\mathbf{q}_3} m_{-\mathbf{q}_4} m_{-\mathbf{q}_5} m_{-\mathbf{q}_6} \rangle \delta_{\mathbf{q}_1+\mathbf{q}_2+\mathbf{q}_3+\mathbf{q}_4+\mathbf{q}_5+\mathbf{q}_6,0} \right. \\ &\quad \left. \left. - 3 \langle m_{-\mathbf{q}_1} m_{-\mathbf{q}_2} \rangle \delta_{\mathbf{q}_1+\mathbf{q}_2,0} \left(5 \langle m_{-\mathbf{q}_3} m_{-\mathbf{q}_4} m_{-\mathbf{q}_5} m_{-\mathbf{q}_6} \rangle \delta_{\mathbf{q}_3+\mathbf{q}_4+\mathbf{q}_5+\mathbf{q}_6,0} \right. \right. \right. \\ &\quad \left. \left. \left. - 6 \langle m_{-\mathbf{q}_3} m_{-\mathbf{q}_4} \rangle \langle m_{-\mathbf{q}_5} m_{-\mathbf{q}_6} \rangle \delta_{\mathbf{q}_3+\mathbf{q}_4,0} \delta_{\mathbf{q}_5+\mathbf{q}_6,0} \right) \right] \right\}. \end{aligned} \quad (\text{C2})$$

-
- * E-mail: kjetil.borkje(a)phys.ntnu.no
† E-mail: steinar.kragset(a)phys.ntnu.no
‡ E-mail: asle.sudbo(a)phys.ntnu.no
- ¹ I. Affleck and J. B. Marston, Phys. Rev. B **39**, 11538 (1989).
 - ² G. Baskaran and P. W. Anderson, Phys. Rev. B **37**, 580 (1988).
 - ³ I. Affleck, Z. Zou, T. Hsu and P. W. Anderson, Phys. Rev. B **38**, 745 (1988); Z. Zou and P. W. Anderson, Phys. Rev. B **37**, 627 (1988).
 - ⁴ E. Dagotto, E. Fradkin and A. Moreo, Phys. Rev. B **38**, 2926 (1988).
 - ⁵ L. B. Ioffe and A. I. Larkin, Phys. Rev. B **39**, 8988 (1989).
 - ⁶ N. Nagaosa and P. A. Lee, Phys. Rev. B **61**, 9166 (2000).
 - ⁷ G. Mudry and E. Fradkin, Phys. Rev. B **49**, 5200 (1994); *ibid.* **50**, 11409 (1994).
 - ⁸ I. Ichinose and T. Matsui, Phys. Rev. B **51**, 11860 (1995); I. Ichinose, T. Matsui and M. Onoda, Phys. Rev. B **64**, 104516 (2001).
 - ⁹ D. K. K. Lee and Y. Chen, J. Phys. A: Math. Gen. **21**, 4155 (1988).
 - ¹⁰ T. Senthil and M. P. A. Fisher, Phys. Rev. B **62**, 7850 (2000).
 - ¹¹ A. M. Polyakov, Nucl. Phys. B **120**, 429 (1977).
 - ¹² J. M. Kosterlitz, J. Phys. C **10**, 1046 (1977).
 - ¹³ I. F. Herbut and Z. Tešanović, Phys. Rev. Lett. **76**, 4588 (1996).
 - ¹⁴ H. Kleinert, F. S. Nogueira, and A. Sudbø, Phys. Rev. Lett. **88** 232001 (2002); Nucl. Phys. B **666** 361-395 (2003).
 - ¹⁵ M. Hermele, T. Senthil, M. P. A. Fisher, P. A. Lee, N. Nagaosa and X.-G. Wen, cond-mat/0404751.
 - ¹⁶ I. F. Herbut and B. H. Seradjeh, Phys. Rev. Lett. **91**, 171601 (2003); I. F. Herbut, B. H. Seradjeh, S. Sachdev and G. Murthy, Phys. Rev. B **68**, 195110 (2003); M. J. Case, B. H. Seradjeh and I. F. Herbut, Nucl. Phys. B **676** 572-586 (2004).
 - ¹⁷ M. N. Chernodub, E.-M. Ilgenfritz and A. Schiller, Phys. Lett. B **547**, 269 (2002); *ibid.* **555**, 206 (2003).
 - ¹⁸ S. Kragset, F. S. Nogueira, and A. Sudbø, Phys. Rev. Lett. **92** 186403 (2004).
 - ¹⁹ D. R. Nelson and J. M. Kosterlitz, Phys. Rev. Lett. **39**, 1201 (1977); P. Minnhagen and G. G. Warren, Phys. Rev. B **24**, 2526 (1981).
 - ²⁰ P. Minnhagen and B. J. Kim, Phys. Rev. B **67**, 172509 (2003).
 - ²¹ A. M. Ferrenberg and R. H. Swendsen, Phys. Rev. Lett. **61** 2635 (1988); Phys. Rev. Lett. **63** 1195 (1989).
 - ²² J. M. Kosterlitz and D. J. Thouless, J. Phys. C **6**, 1181 (1973).
 - ²³ H. A. Fertig and J. P. Straley, Phys. Rev. B **66**, 201402(R) 2002; H. A. Fertig, Phys. Rev. Lett., **89**, 035703 (2002).
 - ²⁴ P. Olsson, private communication.
 - ²⁵ J. M. Kosterlitz, J. Phys. C **10**, 3753 (1977).
 - ²⁶ P. Minnhagen, Phys. Rev. B **32**, 3088 (1985).